doi:10.1016/j.jmb.2004.03.074 J. Mol. Biol. (2004) 339, 447–458

JMB

Available online at www.sciencedirect.com

SCIENCE DIRECT®

ELSEVIER

Mutational Analysis of the Energetics of the GrpE·DnaK Binding Interface: Equilibrium Association Constants by Sedimentation Velocity Analytical Ultracentrifugation

Amy D. Gelinas, Joseph Toth, Kelley A. Bethoney, Walter F. Stafford and Celia J. Harrison*

Boston Biomedical Research Institute, 64 Grove St. Watertown, MA 02472, USA

DnaK, the prokaryotic Hsp70 molecular chaperone, requires the nucleotide exchange factor and heat shock protein GrpE to release ADP. GrpE and DnaK are tightly associated molecules with an extensive protein–protein interface, and in the absence of ADP, the dissociation constant for GrpE and DnaK is in the low nanomolar range. GrpE reduces the affinity of DnaK for ADP, and the reciprocal linkage is also true: ADP reduces the affinity of DnaK for GrpE. The energetic contributions of GrpE side-chains to GrpE–DnaK binding were probed by alanine-scanning mutagenesis. Sedimentation velocity (SV) analytical ultracentrifugation (AUC) was used to measure the equilibrium constants (K_{eq}) for GrpE binding to the ATPase domain of DnaK in the presence of ADP. ADP-bound DnaK is the natural target of GrpE, and the addition of ADP (final concentration of 5 μM) to the preformed GrpE–$DnaK_{ATPase}$ complexes allowed the equilibrium association constants to be brought into an experimentally accessible range. Under these experimental conditions, the substitution of one single GrpE amino acid residue, arginine 183 with alanine, resulted in a GrpE–$DnaK_{ATPase}$ complex that was weakly associated ($K_{eq} = 9.4 \times 10^4$ M). This residue has been previously shown to be part of a thermodynamic linkage between two structural domains of GrpE: the thermosensing long helices and the C-terminal β-domains. Several other GrpE side-chains were found to have a significant change in the free energy of binding ($\Delta\Delta G \sim 1.5$ to 1.7 kcal mol^{-1}), compared to wild-type GrpE·$DnaK_{ATPase}$ in the same experimental conditions. Overall, the strong interactions between GrpE and DnaK appear to be dominated by electrostatics, not unlike barnase and barstar, another well-characterized protein–protein interaction. GrpE, an inherent thermosensor, exhibits non-Arrhenius behavior with respect to its nucleotide exchange function at bacterial heat shock temperatures, and mutation of several solvent-exposed side-chains located along the thermosensing indicated that these residues are indeed important for GrpE–DnaK interactions.

Keywords: analytical ultracentrifugation; molecular chaperone; protein–protein interaction; alanine-scanning mutagenesis; equilibrium association constants

*Corresponding author

Abbreviations used: AUC, analytical ultracentrifugation; *s*, sedimentation coefficient; S, a unit of svedberg (10^{-13} seconds); SV, sedimentation velocity; K_{eq}, equilibrium binding constant; K_d, dissociation constant; wt, wild-type; DSC, differential scanning calorimetry; T_m, midpoint temperature of thermal transition; ATPase, adenosine 5′-triphosphate hydrolase; GDP, guanosine 5′-diphosphate.

E-mail address of the corresponding author: harrison@bbri.org

Introduction

Molecular chaperones are a diverse family of proteins that function to protect proteins in the intracellular millieu from irreversible aggregation during synthesis and in times of cellular stress. The bacterial molecular chaperone DnaK is an enzyme that couples cycles of ATP binding, hydrolysis, and ADP release by an N-terminal ATP-hydrolyzing domain to cycles of sequestration and release of unfolded proteins by a C-terminal substrate binding domain.[1–3] The substrates of DnaK and its well known eukaryotic homologs Hsp70 and BiP include nascent polypeptides emerging from ribosomes, proteins being translocated to the mitochondria, proteins being transported across membranes, and proteins unfolded by cellular stress.

Dimeric GrpE is the co-chaperone for DnaK, and acts as a nucleotide exchange factor, stimulating the rate of ADP release 5000-fold.[4,5] DnaK is itself a weak ATPase; ATP hydrolysis by DnaK is stimulated by its interaction with another co-chaperone, DnaJ. Thus the co-chaperones DnaJ and GrpE are capable of tightly regulating the nucleotide-bound and substrate-bound state of DnaK in ways that are necessary for the normal housekeeping functions and stress-related functions of the DnaK molecular chaperone cycle. In addition, the intrinsic thermal stability of the long helices of GrpE give the molecule the properties of a thermosensor. At higher temperatures relevant to heat shock, GrpE's function as a nucleotide exchange factor decreases in a non-Arrhenius fashion,[6,7] favoring DnaK·ADP and retention of the unfolded polypeptide substrate.[8] Finally, GrpE has an additional role in augmenting peptide release of substrates from the DnaK substrate binding domain in an ATP-independent manner.[9–11]

The X-ray crystal structure of GrpE in complex with the ATPase domain of DnaK revealed that GrpE is an asymmetric homodimer, bent in a manner that favors extensive contacts with only one $DnaK_{ATPase}$ monomer.[9] GrpE and DnaK associate tightly in the absence of nucleotide, which is consistent with the X-ray crystal structure that revealed more than 2800 $Å^2$ of buried surface area in the complex of these two proteins.[9,12,13] Previously reported dissociation constants are in reasonable agreement; a K_d of 30 nM was determined by surface plasmon resonance (SPR) techniques[9] and a K_d of 1 nM was deduced by kinetic analyses.[5] The X-ray structure showed that GrpE does not actively compete for the atomic positions occupied by the nucleotide.[9] GrpE and ADP mutually reduce one another's affinity for DnaK 200-fold,[5] and ATP instantly dissociates GrpE from DnaK with a rate too fast to be measured by SPR.[9] This reciprocally linked relationship between nucleotide affinity and the affinity of nucleotide exchange factor for its cognate nucleotide hydrolase has been seen in other systems. For example, a transient tertiary complex between RCC1 (the guanine exchange factor), Ran (cognate GTPase) and GDP has been observed by kinetic analyses.[14] Similarly, a transient ternary complex of GrpE·DnaK·ADP has been detected using fluorescent kinetic techniques.[5]

In the X-ray structure of the complex of dimeric GrpE with the ATPase domain of DnaK, a total of 18 potentially important protein–protein contacts can be identified, but which of the observed side-chain interactions are directly relevant for high-affinity GrpE–DnaK interactions, or for GrpE's function as a temperature-dependent nucleotide exchange factor? As a nucleotide exchange factor, GrpE must actively recognize the ADP state of DnaK, yet bind to and stabilize the open, nucleotide-free conformation of DnaK and be readily displaced by ATP, the latter of which coordinates the re-closing of the deep nucleotide binding cleft. To probe the molecular mechanisms of the molecular chaperone cycle, GrpE, the ATPase domain of DnaK, and ADP were studied under equilibrium conditions to examine the relevant energetic contributions of GrpE side-chains to protein–protein recognition at the GrpE–DnaK interface.

The perturbation of protein–protein interactions by alanine-scanning mutagenesis has proven to be a fruitful method for elucidating the functional binding epitope between two proteins.[15] Some of the better known studies include hGH·hGHbp[16] and HEL·HyHEL-63,[17] which have primarily made use surface plasmon resonance and isothermal titration calorimetry to define the protein interaction hot-spots. From these and other studies, it has become apparent that the distribution of energetically important side-chains in protein–protein interfaces can be as varied and diverse as the proteins themselves. But in general, protein–protein interactions can be dominated by only a few high-energy interactions, with most crystallographically observed residues making insignificant contributions to the total binding energy, or alternatively many residues can contribute smaller binding energies to the functional epitope of binding. $GrpE{\cdot}DnaK_{ATPase}$ appears to fall in to the first general model for protein–protein interactions: the mutation of a few particular amino acids revealed that these side-chains dominate the energetics of binding, and provide further insight into the temperature-dependent functionality of GrpE.

Described here is the application of a significant, new method for the analysis of equilibrium association constants by sedimentation velocity AUC. The relative energetic contributions of side-chains in the GrpE–DnaK binding epitope were compared by using 16 alanine-perturbation mutants (of the 18 GrpE–DnaK contacts, two are already alanine). Time-difference data collected by sedimentation velocity AUC were fit with new methods to find the equilibrium association constants of mutant–GrpE·DnaK complexes.

Results

Hydrodynamic characterization of the individual binding partners

The sedimentation coefficients of GrpE and the $DnaK_{ATPase}$ (DnaK amino acid residues 1–388) domain were determined by sedimentation velocity AUC at 50,000 rpm and at 20 °C using interference optics in a BeckmanCoulter XL-I Analytical Ultracentrifuge (Figure 1). The sedimentation coefficient ($s_{20,b}$) of the 42 kDa monomeric $DnaK_{ATPase}$ domain was determined to be 3.05 svedbergs (S) in the absence of nucleotide, after exhaustive dialysis to remove nucleotide.[18] In the presence of 0.5 μM ADP and 5.0 μM ADP, the sedimentation coefficient was found to be 3.09 S; this difference is within experimental error. Dimeric, wild-type full-length GrpE (expressed with an N-terminal hexahistidine tag, conferred by the bacterial overexpression plasmid pET-15b) had a $s_{20,b}$ of 2.33 S (~46.9 kDa), and showed no concentration dependence of s over a concentration range of 16.6 to 1.8 μmol.[19] Partial specific volumes, v-bar, were calculated from amino acid composition by the method described by Perkins.[20] These values are 0.736 for dimeric, wild-type, His-tagged full-length GrpE, and 0.741 for the $DnaK_{ATPase}$ domain, residues 1–388. A value for the solvent density, ρ, was calculated to be 1.0024 for the buffer used in all experiments at 20 °C (25 mM Mopso (pH 6.8), 100 mM NaCl, 1 mM $MgCl_2$, 1 mM $CaCl_2$). The correction factor, including the buoyancy (1.0120) and viscosity (1.0088) corrections, is $s_{20,w} = (1.02085)\cdot(s_{20,b})$.

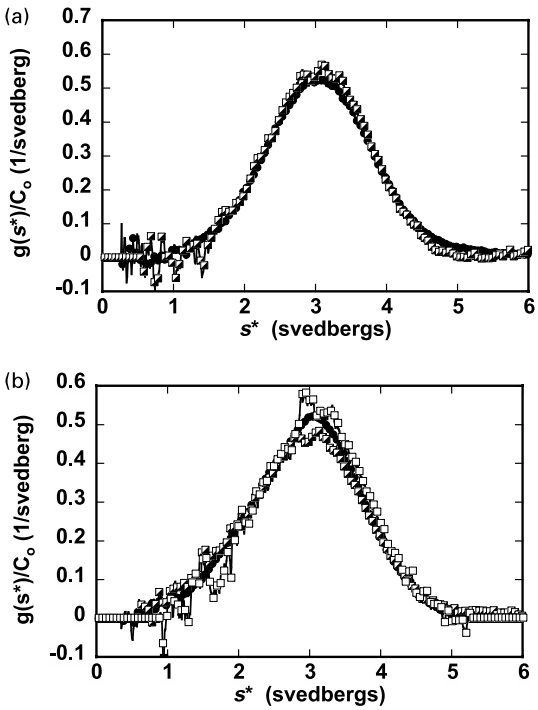

Figure 1. (a) Time-derivative ($g(s^*)$) plot of nucleotide-free $DnaK_{ATPase}$, indicating a sedimentation coefficient of 3.05 S. The loading concentrations (shown normalized) were found to be as follows: 4.1 μM (filled circles) and 1.2 μM (half-filled squares). (b) Time-derivative plot of $DnaK_{ATPase}$ in the presence of 5 μM ADP ($s_{20,b} = 3.09$ S). The loading concentrations (shown normalized) were found to be as follows: 14.4 μM (filled circles), 4.8 μM (half-filled squares) and 1.4 μM (open squares). No concentration dependence to the sedimentation coefficient was observed over this protein concentration range for either nucleotide-free $DnaK_{ATPase}$ or $DnaK_{ATPase}$ in the presence of 5.0 μM ADP. Data were collected using interference optics with a BeckmanCoulter XL-I at 50,000 rpm and at a temperature of 20 °C. Data were analyzed with DCDT.[21]

Hydrodynamic characterization of the GrpE–$DnaK_{ATPase}$ complex

The GrpE–DnaK complex is tightly associated in the absence of nucleotide; dissociation could not be observed in the analytical ultracentrifuge, even upon dilution to 0.15 μM, in the standard buffer condition containing 0.1 M NaCl and at 20 °C (data not shown). High ionic strength (0.5 M NaCl, 20 °C) and low temperature (4 °C, 0.1 M NaCl) did not cause complex dissociation upon dilution of the protein complex to 0.15 μM (data not shown). A mutant complex, GrpE(V192A)–$DnaK_{ATPase}$, was used to investigate dissociation as a function of ADP concentration at 0.5 μM, 5.0 μM, 50 μM, and 500 μM (Figure 2). An intermediate concentration of 5 μM ADP resulted in a shift in the peak observed in the $g(s^*)$ plot from 4.07 S to 3.35 S, indicating significant, but not total, dissociation of the GrpE–DnaK complex. Therefore 5.0 μM ADP was chosen for further studies of the effect of alanine-point mutations on the free energy of GrpE–DnaK associations.

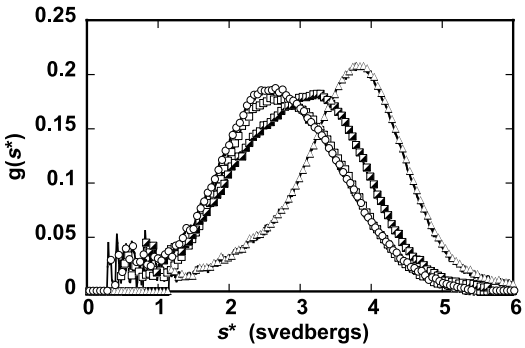

Figure 2. Time-derivative ($g(s^*)$) plot for the V192A mutation of GrpE in complex with $DnaK_{ATPase}$ at various ADP concentrations. The protein loading concentration for each cell was ~1.6 μM, and the ADP concentrations were as follows: 500 μM (open circles), 50 μM (open squares), 5.0 μM (half-filled squares), and 0.5 μM (open triangles). 5.0 μM ADP was used for all analyses.

Free-energy changes of mutant GrpE binding to DnaK

Stoichiometric complexes of 16 mutant GrpE proteins and $DnaK_{ATPase}$ were prepared by gel filtration chromatography.[9] Sedimentation velocity AUC data were collected and analyzed with DCDT,[21] ABCD_Fitter and SEDANAL. Examples of time derivative ($g(s^*)$) data for two mutant complexes and the residual plots for the fits to the corresponding time difference curves for the model A + B = C are shown in Figures 3 and 4.

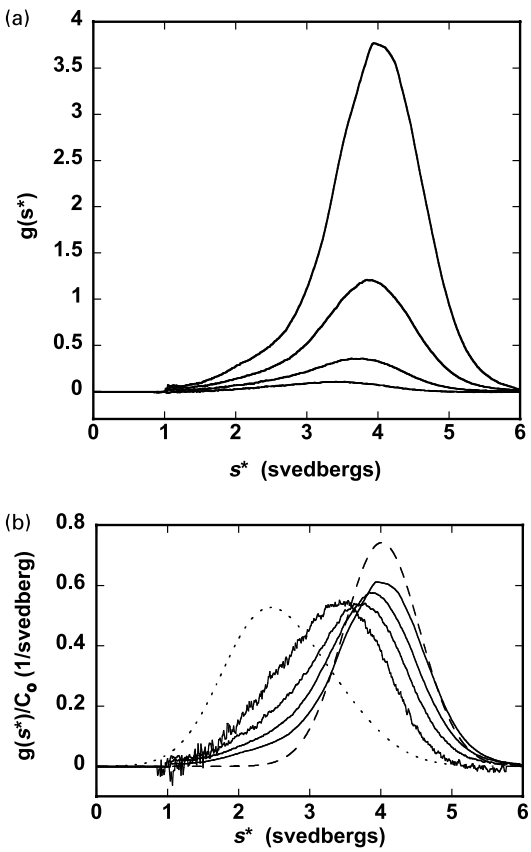

Figure 3. Shown are the raw (a) and normalized (b) time-derivative ($g(s^*)$) plots for GrpE(M189A)·$DnaK_{ATPase}$ in 5.0 μM ADP. As the concentration of the protein decreases, complex dissociation increases. In a, the protein loading concentration for the tallest curve is 1.9 mg ml^{-1}; for each subsequently lower curve the concentrations are 0.6 mg ml^{-1}, 0.2 mg ml^{-1}, and 0.06 mg ml^{-1}, respectively. In b, the same data are shown with the protein loading concentrations normalized. The protein concentration increases from left to right for the four curves represented by continuous lines: 0.06, 0.2, 0.6, and 1.9 mg ml^{-1}. The short-dash curve represents the hypothetical $g(s^*)$ plot for a 1 : 1 stoichiometry of dimeric GrpE and $DnaK_{ATPase}$ that are non-interacting; the long-dash curve is a hypothetical $g(s^*)$ plot for a stoichiometric complex of dimeric GrpE and $DnaK_{ATPase}$ that are fully associated. Curve fitting the time difference data to find numerical solutions to the Lamm equation directly measures the equilibrium binding constant and the sedimentation coefficient, as well as other variables.

The best-fit K_{eq} constants, sedimentation coefficients, and free-energy changes for 16 GrpE mutant proteins in complex with $DnaK_{ATPase}$ in the presence of 5.0 μM ADP are tabulated in Table 1. One mutant, R183A, was the most disruptive to GrpE–$DnaK_{ATPase}$ binding ($K_{eq} = 9.4 \times 10^4$ M). No other mutation was as disruptive. The thermodynamic properties (measured by differential scanning calorimetry) of R183A and another disruptive mutant, V192A have been reported.[22] Both mutations destabilize the β-domains, shifting the T_m from its normal value of 75 °C downward to 70.1 °C and 64.3 °C, respectively. As in other studies, there is no correlation between the change in free energy of each mutation (from the thermodynamic relationship $\Delta\Delta G = -RT(\ln(K_{WT}/K_{mut}))$ with the change in buried surface area, or the change in buried hydrophobic surface area (data not shown).

Discussion

The energetic contributions of individual GrpE side-chains to the high-affinity GrpE–DnaK interaction were probed by perturbing the interface with alanine substitutions and quantified by measuring the equilibrium constants using a time-difference method for treating sedimentation velocity AUC data. The findings of this study, namely the importance of arginine 183 to GrpE–DnaK interactions as well as several other charged side-chains located along the thermosensing helices of GrpE, and the observed conformational changes of mutant complexes will be discussed below, along with details of the time-difference fitting method.

Structural anatomy of the interaction surface

All three structural domains of GrpE (the long helices, the four-helix bundle, and the β-domains) contribute to the extensive interface formed with three of the four domains of the $DnaK_{ATPase}$ domain. If considered individually, the three major areas of interaction and three minor areas of interaction have no detectable pattern of hydrophobic and hydrophilic residues. When viewed on a whole, the complex of GrpE–$DnaK_{ATPase}$ generally follows the common pattern found at protein–protein interfaces of hydrophobic residues ringed by charged residues.[23] A total of 11 of the 18 potential GrpE–DnaK contacts reside on the β-domains; the majority are hydrophobic residues. Outside of the compact β-domains, all but one of the rest of the GrpE·$DnaK_{ATPase}$ interactions are charged residues that make salt bridges or hydrogen bonds to DnaK. Of the 18 potential GrpE–DnaK interactions, 16 are mutable; two are already alanine. The three major areas of interaction are area I (red in Figure 5) in which residues from the top of the four-helix bundle of GrpE contact domain IIB of $DnaK_{ATPase}$, away from the deep

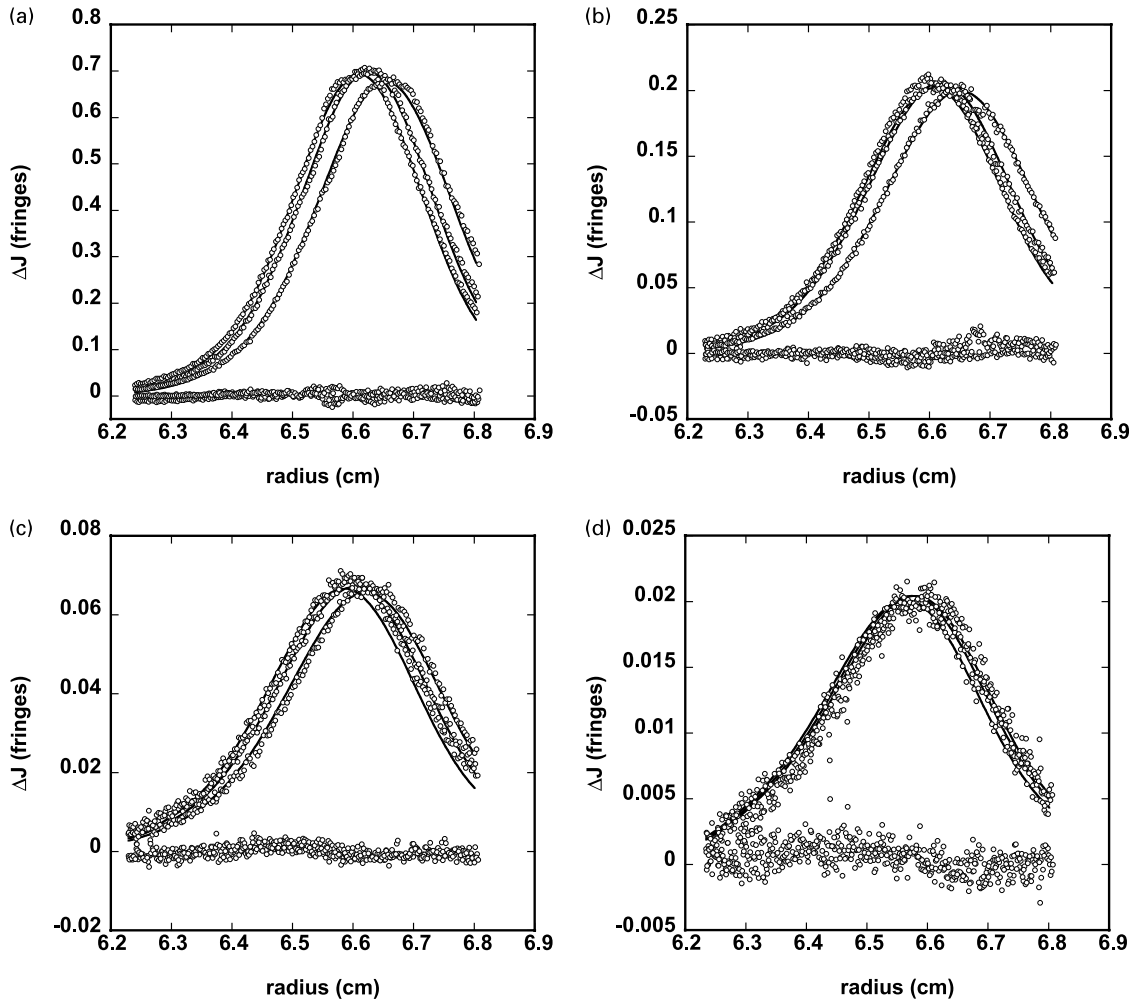

Figure 4. Time-difference residual plot for each of the four concentrations of GrpE(E107A)·DnaK$_{ATPase}$ in the presence 5.0 μM ADP. Shown are raw data (open circles), the corresponding model (continuous lines), and the residuals of the fit (open circles) for three of the 21 pairs of scans taken over time. The data were truncated at one side to avoid the contribution of aggregates to the data. Time-differences (ΔJ, on the y axis) are expressed in units of optical fringes. The loading protein concentrations for each of the four cells were: (a) 14.7 μM, (b) 4.7 μM, (c) 1.7 μM, and (d) 0.58 μM.

Table 1. Equilibrium association constants, complex sedimentation coefficients and changes in the free energy of binding for mutant GrpEs in complex with the ATPase domain of DnaK, at 20 °C

GrpE	S_C GrpE·DnaK·ADP (svedbergs)	K_{eq}	$\Delta G_{20\,°C}$ (kcal mol^{-1})	$\Delta G_{mutant} - \Delta G_{wild\text{-}type}$ (kcal mol^{-1})
R183A	4.0	9.4×10^4 M	−6.6	2.2
R73A	4.3	2.3×10^5 M	−7.2	1.7
K82A	4.4	2.4×10^5 M	−7.2	1.7
P151A	4.3	3.3×10^5 M	−7.4	1.5
V192A	4.1	3.7×10^5 M	−7.5	1.4
M159A	4.2	4.0×10^5 M	−7.5	1.4
R74A	4.4	5.0×10^5 M	−7.6	1.3
R104A	4.1	5.2×10^5 M	−7.7	1.2
M189A	4.4	6.3×10^5 M	−7.8	1.1
I157A	4.0	6.4×10^5 M	−7.8	1.1
R186A	4.2	1.2×10^6 M	−8.1	0.8
E107A	4.1	1.7×10^6 M	−8.4	0.4
Q155A	4.0	1.9×10^6 M	−8.4	0.4
L149A	4.0	2.5×10^6 M	−8.6	0.2
V108A	3.9	4.3×10^6 M	−8.9	∼0
M174A	4.0	4.6×10^6 M	−8.9	∼0
wild type	4.1	4.7×10^6 M	−8.9	*datum*

The free energy changes in GrpE–DnaK binding are given by the relationship $\Delta\Delta G = -RT \ln (K_{WT}/K_{MUT})$, where K_{WT} is the K_{eq} for wild-type GrpE and DnaK$_{ATPase}$ in 5.0 μM ADP, and K_{MUT} is for mutant GrpEs in reversible association with DnaK$_{ATPase}$, in the identical conditions. R183A was fit with a kinetic model due to a slow reaction boundary.

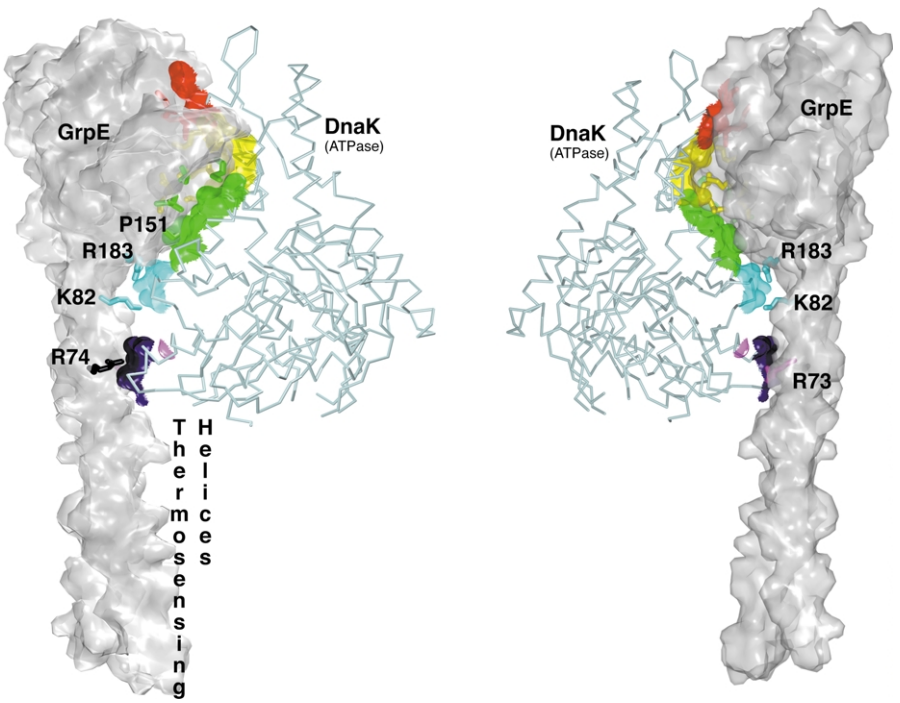

Figure 5. Representation of the GrpE–DnaK$_{ATPase}$ complex, based on the co-crystal (PDB I.D. code is 1DKG[9]). GrpE is drawn as a semi-transparent molecular surface, and DnaK$_{ATPase}$ is drawn as an α-carbon trace. The right-hand view is the reverse side of the left-hand view. The side-chains of GrpE that make contact to DnaK were not included in the calculation of the GrpE molecular surface, and so they appear to stick out. In the interest of clarity, most side-chains of GrpE are not labelled. The thermosensing helices are indicated. Shown in color are the interacting molecular surfaces of DnaK that are calculated to be within five Å of the GrpE side-chains that were mutated in this study. The GrpE side-chains and the DnaK "eggshell" surfaces are colored as described in the text and as follows. Area I (red) GrpE R104, E107, and V108. Area II (yellow) GrpE Q155, I157, M174, R186, and M189. Area III (green) L149, P151, M159, V192. Area IV (cyan) K82, R183. Area V (indigo) GrpE R74 (proximal helix). Area VI (violet) R73 (distal helix). This Figure was made with unpublished software (D. Jeruzalmi), Molscript,[33] and POVRAY (http://www.povray.org).

cleft of DnaK$_{ATPase}$; area II (yellow in Figure 5), in which GrpE residues from the proximal β-domain of GrpE contact the DnaK$_{ATPase}$ domain IIB side of the cleft; and area III (green in Figure 5), in which GrpE residues from the β-domain contact the DnaK$_{ATPase}$ domain IB side of the nucleotide binding cleft. The three minor areas of interaction essentially amount to only charged residues that are fully solvent-exposed (except Arg183). These areas are arrayed along the C-terminal half of the long α-helices of GrpE. They are: area IV (cyan), the "armpit" of GrpE contacting a loop in DnaK domain IA; area V (indigo), in which a single arginine (74) contacts some DnaK backbone atoms; and area VI (violet), in which a single arginine (73) from the distal GrpE monomer makes few contacts to DnaK. The latter is the only side-chain from the distal GrpE monomer to make a potential contact to DnaK.

Equilibrium constants for alanine-perturbation mutants

One alanine-perturbation mutation of GrpE, R183A, appeared quite deleterious to GrpE–DnaK binding. That is, the mutant complex GrpE(R183A)–DnaK$_{ATPase}$ was only weakly associated, with an equilibrium constant of 9×10^4 M in the presence of 5.0 μM ADP. In fact, dissociation of GrpE(R183A)–DnaK$_{ATPase}$ could also be seen in the absence of nucleotide, by observing the shift in the peaks in the time-derivative plots of a dilution series (akin to Figure 3(a) and (b); data not shown). By way of contrast, no other mutant or wild-type GrpE–DnaK complex dissociates upon dilution (to the typical limit of experimental detectablity, around 500 nM), in the absence of nucleotide (data not shown). GrpE reduces the affinity of DnaK for ADP, and in a thermodynamically linked manner, ADP destabilizes the GrpE–DnaK complex, yet not to the same extent that ATP does, which has the effect of instantaneously causing GrpE to dissociate from DnaK. Here, the use of an experimentally optimal concentration of ADP, 5.0 μM (Figure 2), augmented GrpE–DnaK dissociation to the extent that the equilibrium constants were readily ascertained from the data.

The equilibrium association constant for the GrpE(R183A)–DnaK$_{ATPase}$ complex ($K_{eq} \sim 9.4 \times 10^4$ M; the inverse, K_d, thus is 1.1×10^{-5} M^{-1}) corresponds to a change in the free energy of binding between this mutant and wild-type of ~2.2 kcal mol^{-1}. By comparison to other studies of protein–protein interactions, this change

in free energy is large enough to be deemed a protein interaction hot spot. However, since there are only two atomic interactions between R183 and DnaK visible in the crystal structure, it seems necessary to also consider the thermodynamic consequences of the R183A mutation. In the monomer of GrpE proximal to DnaK, arginine 183 extends from the base of the β-domain towards the long helix of GrpE, making a contact to the carbonyl oxygen of DnaK residue 28 *via* its ε amino group, and to an ε oxygen of DnaK's Glu31 *via* one of its η nitrogen atoms. These two DnaK residues are part of a loop, that when deleted, abrogates GrpE binding.[24] In addition, the aliphatic portion of the long Arg side-chain packs on top of the ring of phenylanine 86, which sits at the break between the long helix of GrpE and the four-helix bundle. All told, Arg183 makes as many intramolecular contacts within GrpE as it does with DnaK. Moreover, it has been previously shown that mutation of Arg183 to alanine causes a destabilization of the β-domain, and is an integral part of the thermodynamic linkage that transmits information from the thermosensing long helices to the GrpE β-domains.[22] Thus, the perturbation of Arg183 to alanine not only has thermodynamic consequences, but these thermodynamic effects combine with the loss of the atomic contacts with DnaK to create the strongly deleterious effect upon GrpE–DnaK binding. As for the wild-type GrpE–$DnaK_{ATPase}$ complex, Reinstein and co-workers reported that in the presence of excess ADP, GrpE has a 200-fold reduced affinity for DnaK.[5] Using Reinstein's K_d for GrpE–DnaK of ~1 nM, a 200-fold decrease in the affinity of wild-type GrpE would be raise the K_d to ~200 nM, or an approximate K_{eq} of 5×10^6 M, which is quite similar to the value of 4.6×10^6 M that is obtained in this analysis in the presence of 5 μM ADP, the latter of which is generally two to five times greater than the highest protein concentration used in the analyses (the K_d for ADP binding to DnaK is ~90 nM.[5])

The changes in free energy of binding for 15 other mutant GrpEs (compared to the wild-type GrpE) to $DnaK_{ATPase}$ were also measured in 5.0 μM ADP, and are reported in Table 1. The range in K_{eq} varied from 2.3×10^5 (R73A) to 4.6×10^6 (M174A), while the wild-type GrpE–$DnaK_{ATPase}$ was found to be 4.6×10^6. This ~20-fold difference in K_{eq} from 2.3×10^5 to 4.6×10^6 corresponds to a range in $\Delta\Delta G$ of -1.7 kcal mol^{-1}. Those side-chains, when mutated to alanine, which have decreased affinity on the order of $\sim 1 - 2$ kcal mol^{-1} can only be considered moderately important for interaction in other protein–protein model systems, whereas a strongly interacting side-chain would contribute a $\Delta\Delta G$ of 3.5 kcal mol^{-1} when perturbed to alanine, compared to wild-type binding.[15] It has been observed that tryptophan, tyrosine, and arginine are generally over-represented in protein interaction hot spots.[15] There are no tyrosine or tryptophan residues at the GrpE–DnaK interface, but arginine residues do account for four of the 18 GrpE side-chains that contact DnaK; the dominance of Arg183 has already been discussed.

Aside from R183A, another mutation known to alter the thermodynamic properties of GrpE (V192A) was investigated as part of this study. Previously it was shown that like R183A, the V192A mutation destabilized the GrpE β-domains, shifting the midpoint of the thermal unfolding transition from 75.2 °C to 64.3 °C.[22] The β-domains of GrpE are quite compact; 55 residues contribute to a well-folded entity that has a minimal hydrophobic core of four residues, one of which is V192, which is quite buried in the unbound GrpE monomer. Yet one of the γ methyl groups of V192 is within 4 Å of a γ methyl group of T60 on DnaK, which raises the possibility of van der Waal's interactions. Mutation of V192 to alanine, which demonstrably disrupts thermal stability of the β-domain, ultimately affects GrpE–DnaK binding as well, though not to the same degree as R183A, which has a similar thermodynamic phenotype. Perhaps this is due to an overall destabilization that effects the 11 weaker GrpE–DnaK contacts found on the β-domain. This calls attention to the role that thermodynamic destabilization of a binding partner may play in affecting protein–protein interactions.

Three charged amino acid residues along the long helices of GrpE appear to contribute more to the energetics of GrpE–DnaK binding than the bulk of the hydrophobic residues located on the β-domains. These residues, Lys82, Arg74, and Arg73 are fairly well exposed to bulk solvent in the crystal structure of GrpE–$DnaK_{ATPase}$, and generally cause loss of a little more than one order of magnitude in the equilibrium constant, which corresponds to about 1.5 kcal mol^{-1}. Compared to other protein–protein interaction studies, a free energy change of 1.5 kcal mol^{-1} is not very significant, yet these solvent-exposed residues do affect the affinity, and actually have a greater effect on binding than does the alanine perturbation of many of the hydrophobic residues that are protected from solvent when the β-domains bind DnaK (see Table 1). It can be seen in the GrpE–$DnaK_{ATPase}$ co-crystal that Arg73, Arg74 and Lys82 make salt bridges, hydrogen bonds, or (presumably) water-mediated contacts to DnaK (Figure 5). The side-chains on the long helix proximal to DnaK are all in different conformations than their counterparts on the long helix distal to DnaK. The conclusion could be drawn that in the absence of DnaK these are well solvated side-chains with the normal range of conformational freedom allowed to those residues. Arginine 73 is potentially used by both GrpE monomers to contact DnaK; this is the only potential contact from the distal GrpE monomer to DnaK observed in the crystal structure. It could be that the interactions between these residues and their cognate atomic partners on DnaK may be influenced by the thermal unfolding of the long helices at temperatures relevant to heat shock. It has been shown that the long helices

of GrpE undergo a helix-to-coil unfolding process, and this unfolding is responsible for the observed non-Arrhenius temperature dependence of GrpE's function as a nucleotide exchange factor.[6,7,22] The thermodynamic properties of these three mutants have not yet been studied, so the change in binding affinity cannot be wholly ascribed to the loss of the charged amino groups, *versus* the possible contribution that thermal destabilization of the long helices *via* any one of the three point mutations may have in reducing GrpE–DnaK affinity. Thus, the alanine-perturbation study of GrpE–DnaK contacts along the long helices has provided an insight into the thermosensor hypothesis by revealing that the solvent-exposed side-chains at the interface between the long helices of GrpE and DnaK are part of the functional binding interface.

The remaining GrpE–DnaK contacts not yet discussed are located on the β-domains and on one helix of the four-helix bundle. The equilibrium association constants for these mutants fall in a narrow range from 2.5×10^5 to 4.6×10^6; the latter value is the same equilibrium constant for wild-type GrpE and $DnaK_{ATPase}$ in the 5.0 μM ADP experimental condition. A detailed discussion of each remaining residue will not be presented, but the general trend that the hydrophobic residues appear to be less important than some of the charged residues is obvious. While considerable amount of surface area is buried upon GrpE–DnaK binding, there is no correlation between the change in accessible surface area, or even change in accessible hydrophobic surface area and change in free-energy for the alanine-perturbation mutants (data used to assess the correlation are not shown). In fact, only one amino acid, Ile157, is wholly excluded from solvent upon GrpE binding to DnaK, and the change in buried surface area, 84 Å^2, would be expected to result in a change of $\sim$1.7 kcal mol^{-1}, using a relationship of 21 cal mol^{-1} (Å^2)$^{-1}$. The change in free energy of binding for the I157A mutant was $\sim$1.1 kcal mol^{-1} in this study. Yet the numerical value of the equilibrium constant for any one of the GrpE–DnaK mutant complexes tells only part of the story. Sedimentation velocity AUC also gives shape information about the molecular species in solution (see below).

The conformational change induced by GrpE displaces domain IIb of DnaK, allowing nucleotide dissociation.[9] The compact β-domain of GrpE can be likened to a wedge, that forces DnaK subdomains Ib and IIb apart. Augmenting the β-domain, a few amino acid residues (two charged residues and a small hydrophobic residue) located on the four-helix bundle of GrpE also have potential contacts to domain IIb that are evident in the co-crystal structure. Only R104A, which reduces the affinity of the GrpE(R104A)·$DnaK_{ATPase}$ complex ninefold compared to wild-type, has any appreciable effect on GrpE–DnaK binding in this small region, consistent with the observation that arginine residues are well-represented in protein interaction hot spots.[15] The mutation V108A, has a change in the $s_{20,b}$ of the complex, indicative of an expanded quaternary conformation. The nature of that conformational change, and whether it is similar to the other complexes that have somewhat different sedimentation coefficients (see below) is unknown and will be further investigated.

Conformational changes in mutant complexes

The understanding of the molecular process of protein–protein recognition is not simply a matter of measuring the interaction energies of side-chains found at the protein–protein interface. It is necessary to also consider shape complementarity, structural plasticity, and interactions with solvent. Shape complementarity is evident from crystal structure analysis, while the evaluation of structural plasticity requires experimental and theoretical molecular dynamics. Sedimentation velocity AUC allows the researcher to gain shape information about the macromolecules being studied. Given the sedimentation coefficient, in conjunction with known or calculated values for molecular mass, partial specific volume and hydration, information about the molecular shape in solution can be learned. Here, changes in the sedimentation coefficients for the mutant complexes were detected, indicating conformational changes.

The sedimentation coefficient ($s_{20,b}$) of the GrpE·$DnaK_{ATPase}$ complex is 4.08 S ($s_{20,w}$ of 4.17). Sedimentation coefficients found by sedimentation velocity AUC can be used to calculate the apparent solution dimensions of macromolecules. A shape calculation based on this $s_{20,w}$, a value for v-bar of 0.739, a hydration value of 0.427 g g^{-1} (calculated from the data given by Kuntz & Kauzman,[25] and the molecular mass calculated from the sequences) gives an axial ratio of 8 : 1 for the equivalent prolate ellipsoid of revolution. This is in good agreement with the dimensions of the known crystal structure, and the observation that the N-terminal 34 amino acid residues of GrpE are unstructured in solution.[19]

Here, the observed sedimentation coefficients for most complexes of mutant GrpEs with $DnaK_{ATPase}$ were within 3% of the wild-type value of 4.08 S. The approximate level of error typical in determination of sedimentation coefficients of the complex when curve fitting is 3%. However, several mutant complexes had up to a 7% increase in $s_{20,b}$. The sedimentation coefficient is proportional to the molar mass divided by the frictional coefficient. A single alanine point mutant in GrpE introduces a negligible change in molecular mass with respect to wild-type GrpE. Thus if the molar mass remains unchanged and the sedimentation coefficient has changed, then the frictional coefficient must have changed, indicating a conformational change. A change towards a more compact complex (sedimentation coefficient 4.08 S → 4.4 S; $\sim$7% change), represents a change

in the axial ratio to ~6.5 : 1, assuming a prolate ellipsoid. $DnaK_{ATPase}$ is not subjected to the mutational analysis, and thus is not responsible for the observed variation of the $s_{20,b}$ values. The degree of change in the sedimentation coefficient did not correlate with change in affinity. The sedimentation coefficients of certain mutant GrpEs were analyzed in the absence of DnaK, in order to see if the mutations affected the conformation of GrpE alone (data not shown). All the mutants analyzed varied between 2.25 and 2.43 S, values within 3% of the wild-type value. For example, the sedimentation coefficient of GrpE(R183A) was found to be 2.42 S, which corresponds to a more compact structure in solution compared to wild-type. Similarly, the sedimentation coefficient of GrpE(M174A) was found to be 2.41 S, yet these two proteins have markedly different affinities for $DnaK_{ATPase}$, suggesting that no easy conclusion between protein affinity and conformational changes of a binding partner can be made at this time.

The true significance of a discernible change in the sedimentation coefficient is unknown, and this degree of change could arise in at least three ways: (i) through cross-correlation between the values of s_c and K_{eq} during curve-fitting; (ii) aggregates that cannot be readily taken in by the model; (iii) actual changes in the sedimentation coefficient reflecting a conformational change in the mutant complexes. It is likely that some of the mutant data sets will have a minor amount of cross-correlation and aggregation, nevertheless the observed conformational changes are indicative of an interesting process that requires further investigation.

Fitting time difference curves to find the equilibrium constant

GrpE and DnaK form a reversibly associating complex under the conditions studied by sedimentation velocity. Studying protein–protein interactions *via* sedimentation velocity allows a quantitative examination of a system that is in quasi-equilibrium, so long as the reverse rate constant (i.e. the relaxation time for the dissocation of dimeric GrpE from DnaK) is larger than 10^{-3} per second.[26] That is, when the dissociation and association rates are sufficiently fast compared to the movements of the proteins in the ultracentrifuge cell, the system can be considered to be essentially at instantaneous equilibrium. This has been established for this system by using SEDANAL to simulate sedimentation of GrpE–DnaK under conditions of this study for various values of the forward and reverse rate constants corresponding to a particular value of the equilibrium constant (Figure 6). Several data sets were fit for the equilibrium constant both by assuming instantaneous equilibrium and by fitting forward and reverse rate constants; no significant differences were ever detected (except as described below). Here instantaneous equilibrium constants are reported, except for the mutant R183A, for which the kinetic mode

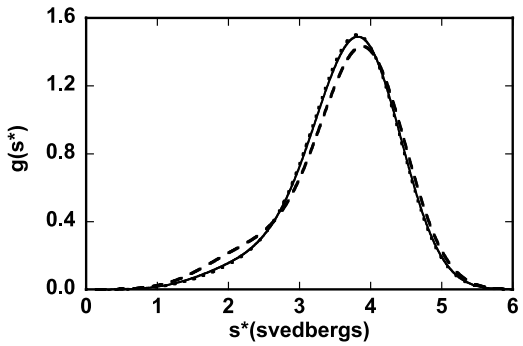

Figure 6. Plot of simulated sedimentation patterns showing the effect of slow reaction kinetics on the shape of the sedimentation profile, for a simulation with the following parameters: $s_A = 2.33$ S; $s_B = 3.09$ S; $s_C = 4.10$ S; $[B]_o/[A]_o = 1.1$; $[A]_o = 1.5 \times 10^{-5}$ M; $K_{eq} = 1 \times 10^6$. In the case of instantaneous equilibrium, simulation yields the continuous line; for the case of $k_r = 1 \times 10^{-3}\ s^{-1}$, the simulation yields the short-dash broken line; for the case where $k_r = 1 \times 10^{-4}\ s^{-1}$, the simulation yields the long-dash broken line. Slow kinetics in this system would not have a significant effect on the shape of the boundary unless k_r was smaller than about $1 \times 10^{-3}\ s^{-1}$; when k_r is at $1 \times 10^{-4}\ s^{-1}$, significant deviations of the sedimentation profile become apparent, which could be modelled by SEDANAL in kinetics mode, if necessary.

of SEDANAL was used, since the $g(s^*)$ plots for GrpE(R183A)–$DnaK_{ATPase}$ had a boundary profile more like a slower reaction than an instantaneous reaction. The calculated rate constants ($k_f = 1.33 \times 10^2\ M^{-1}\ s^{-1}$, and $k_r = 1.41 \times 10^{-3}\ s^{-1}$) resulted in better curve fitting with smaller root mean square differences between the model and the data (data not shown). For all of the other mutants, the equilibrium constants were estimated directly, without curve fitting to find individual rate constants.

The ABCD_fitter and SEDANAL programs were used to fit data according to the simple scheme, A + B = C.[27,28] The model A + B = C can be used to describe the interaction of GrpE and $DnaK_{ATPase}$ in the presence of ADP, because $DnaK_{ATPase}$ and ADP·$DnaK_{ATPase}$ were determined to be hydrodynamically indistinguishable, both experimentally (Figure 1) and theoretically. The following thermodynamic cycle describes the interactions between dimeric GrpE, $DnaK_{ATPase}$ and ADP, with four equilibrium constants (K_1, K_2, K_3, K_4):

$$\begin{array}{ccc} & \overset{K_1}{} & \\ \text{ADP + DnaK} & \rightleftarrows & \text{ADP•DnaK} \\ + & & + \\ \text{GrpE} & & \text{GrpE} \\ K_3 \ \| & & \| \ K_2 \\ \text{ADP + DnaK•GrpE} & \rightleftarrows & \text{ADP•DnaK•GrpE} \\ & \underset{K_4}{} & \end{array}$$

The thermodynamic scheme shown is occurring inside the centrifuge cell, but because the ADP-bound species are hydrodynamically indistinguishable from the ADP-free species, the observed equilibrium constant, K_{eq}, is given by equation (1), and can be reduced to equation (2):

$$K_{eq} = \frac{[\text{DnaK·GrpE}] + [\text{DnaK·ADP·GrpE}]}{([\text{DnaK}] + [\text{DnaK·ADP}])[\text{GrpE}]} \quad (1)$$

$$K_{eq} = K_3\left(\frac{(1 + K_4[\text{ADP}])}{(1 + K_1[\text{ADP}])}\right) \quad (2)$$

Because equation (2) is true, the $\Delta\Delta G$s measured from K_{eq} correspond to the reaction described by K_3 at constant ADP concentration.

For the theoretical calculations, a "bead model" was used to estimate the sedimentation coefficient of the nucleotide-free conformation of $DnaK_{ATPase}$.[29] The theoretical model of nucleotide-free $DnaK_{ATPase}$ is based on the crystal structure of $GrpE{\cdot}DnaK_{ATPase}$, with the explicit assumption that the nucleotide-free conformation of $DnaK_{ATPase}$ in solution closely resembles the nucleotide-free conformation of $DnaK_{ATPase}$ found in the complex crystal structure. The bead model for the nucleotide-bound $DnaK_{ATPase}$ is based on the $HSC70_{ATPase}$ crystal structure, after superimposing $DnaK_{ATPase}$ onto $HSC70_{ATPase}$ as described by Harrison *et al.*[9] and then by "breaking bonds" and superimposing DnaK domain IIB upon domain IIB of the ADP-bound $HSC70_{ATPase}$ domain. These two bead models had theoretical sedimentation coefficients that differed by only 0.3%.

The limits of detectability in the analytical ultracentrifuge are determined by the lowest observable mass concentration. Since the optics of the centrifuge give mass concentrations, the range of experimentally accessible equilibrium constants using the time-difference technique described here is determined by the molecular masses of the species involved. Proteins with higher molecular mass will allow one to detect material at lower molar concentrations for any given mass concentration. The practical lower limit of the interference optics is about 0.01 g l^{-1} and therefore a protein with a molar mass of 100,000 g mol^{-1} can be detected at 0.1 μM, putting the upper limit for the association constant around 1×10^7 M^{-1}. At the other end of the scale, in principal, the upper limit, determined by the magnitude of the concentration gradient, is about 50–100 g l^{-1}, which corresponds to 1 mM for a 100,000 g mol^{-1} protein. In practice, the hydrodynamic and thermodynamic non-ideality of the system at the highest protein concentrations will make it very difficult to analyze the data. A practical upper limit is about 10 g l^{-1} (0.1 mM), corresponding to an association constant of 1×10^4 M^{-1}.

Summary

In summary, the binding energetics of the GrpE–DnaK interface is dominated by arginine 183, the complex of which ($GrpE(R183A)–DnaK_{ATPase}$) is weakly associated, $K_{eq} = 9.4 \times 10^4$ M, which corresponds to a $\Delta\Delta G$ (i.e. $\Delta G_{mutant} - \Delta G_{wild\text{-}type}$) of ~2.3 kcal mol^{-1}, all in the presence of 5 μM ADP. The balance of the GrpE–DnaK interactions contribute less than 2 kcal mol^{-1} to the free energy of binding in the presence of 5 μM ADP, compared to the wild-type complex. It is noted that a complex of $GrpE(R183A)–DnaK_{ATPase}$, even in the absence of ADP, showed dissociation upon dilution to lower protein concentrations, as seen by the shift in the sedimentation coefficients in the $g(s^*)$ plots. However, in the absence of ADP, even the second most destabilizing mutation, V192A, did not have any concentration dependence to the weight-average sedimentation coefficient, which implies that the K_{eq} is around 10^8 (at least) in the absence of ADP. Thus it was necessary to augment GrpE–DnaK dissociation with ADP to quantify the effects of alanine-perturbation on the equilibrium constants. The thermodynamic properties of the R183A and V192A mutants had already been investigated, and it is likely that thermal destabilization is in part responsible for the significant changes in the free energy of GrpE–DnaK interactions. Three solvent-exposed side-chains located along GrpE's thermosensing helices (K82, R73, and R74) were found to be at least as important for the balance of the functional epitope of GrpE–DnaK binding as the numerous hydrophobic side-chains located on the β-domains, which wedge open the nucleotide binding cleft of DnaK. This implicates these charged residues in the non-Arrhenius behavior of GrpE as a nucleotide exchange factor, and implies that these solvent-exposed residues may bind cooperatively with DnaK, rather than simply having an additive effect on the free-energy of GrpE–DnaK binding.[30,31]

Methods

Alanine-perturbation mutants

Alanine-perturbation mutations of GrpE were introduced by PCR-based mutagenesis and sequenced. Mutant GrpEs were overexpressed and purified as described for wild-type GrpE.[19] $DnaK_{ATPase}$ was overexpressed and purified, and complexed with GrpE as described for the preparation of complexes for crystallization.[9] Purified complexes were exhaustively dialyzed *versus* 25 mM Mopso (pH 6.8), 100 mM NaCl, 1 mM $MgCl_2$, 1 mM $CaCl_2$, 5 μM ADP (except for the experiment in Figure 2, in which the ADP was added exogeneously to the sample and reference cells). Three serial threefold dilutions of the starting material were used to span a 27-fold range in protein concentration for all mutants except R183A, for which twofold dilutions were necessary. Sedimentation velocity data were collected on a BeckmanCoulter XLI at 50,000 rpm and 20 °C.

Fitting of the time difference data with ABCD_Fitter and SEDANAL

The programs ABCD_Fitter[27] and SEDANAL[28] was used to fit sedimentation velocity data globally at four different concentrations of the wild-type and mutant GrpE–$DnaK_{ATPase}$ complexes, generally over a constant range of $\omega^2 t(\sim 2.59 \times 10^{11}$ to $\sim 2.95 \times 10^{11})$ using the model A + B = C where A and B are the GrpE dimer and the ATPase domain of DnaK, and C is the heterotrimeric complex, respectively (Figures 3 and 4). The variables fit were: sedimentation coefficient of the complex, s_C; the global association equilibrium constant, K_{eq}; the individual loading concentrations for the cells, C_O; the molar ratio between DnaK and GrpE ($C_{O,B}/C_{O,A}$); the concentration dependence to the frictional coefficient of the complex, K_s; and the weight average second virial coefficient, BM_C. The sedimentation coefficient for the complex of wild-type GrpE with $DnaK_{ATPase}$ (s_C) was found to be 4.08 S in the absence and presence of 5 μM ADP. In most fits the value of s_C was allowed to float, or otherwise was fixed while refining K_{eq}. In practice, K_{eq} and s_C were found to be cross-correlated for tightly associated complexes, and good judgement was required to interpret the results. The other variables of the fits using ABCD_Fitter and SEDANAL include the loading concentration of the cells, C_O, and the ratio between the loading concentration between GrpE and $DnaK_{ATPase}$. In practice, purified complexes of GrpE–$DnaK_{ATPase}$ were dialyzed exhaustively in buffer with a vast excess of 5.0 μmolar ADP and diluted threefold with dialysis buffer serially a total of three times, so that a total of four different protein concentrations (generally over a range of 20 μM to 0.7 μM) at a constant ratio of GrpE to $DnaK_{ATPase}$ were loaded into the sector-shaped ultracentrifuge cells. To reflect the physical reality that the absolute ratio between GrpE and $DnaK_{ATPase}$ cannot change upon dilution, the ratio between GrpE and $DnaK_{ATPase}$ was allowed to float but required to be the same for all four cells for the global fitting. The sizing-column-purified GrpE–$DnaK_{ATPase}$ complexes were nearly stoichiometric; in practice, the refined molar ratio between $DnaK_{ATPase}$ and GrpE varied between 0.7 and 1.3. The refined molar ratio was checked for consistency with the appearance of the complex on a SDS-polyacrylamide gel. ABCD_Fitter and SEDANAL interpolate the data onto an equally spaced (usually 400 point) grid between meniscus and base, after correcting for optical jitter and integral fringe jumps. Using more than 400 data points offered no obvious advantage in convergence of the refined parameters, and significantly increased computation time. In general, for each mutant complex the model was refined until the global root mean square differences between the model and the data were less than 0.01 fringes (3 μg ml^{-1} protein; 3.29 fringes per 1 mg ml^{-1} of protein). ABCD_Fitter was executed on a 1 GHz LINUX box running RedHat 7.2 and SEDANAL was run on a 1.8 GHz Dual processor AMD Athlon running Windows XP Pro.

Bead modelling to calculate theoretical sedimentation coefficients

Bead modelling was carried out using the program HYDRO.[29] Bead models were generated from (i) the crystal structure of $DnaK_{ATPase}$ from the co-crystal with GrpE, 1DKG; (ii) a model of the "closed", nucleotide-bound conformation of $DnaK_{ATPase}$ made by superimposing domain IIB of $DnaK_{ATPase}$ on the position of domain IIB in the 1ATR crystal structure of the bovine brain HSC70 ATPase domain.[32] For each bead model, every amino acid was modelled with a bead of a diameter of ~3.7 Å, centered at the C^{α} position. The exact diameter of the beads was adjusted so that the volume of the model added up to the volume of the hydrated protein. The frictional ratio was calculated as $f/f_o = (s_o/s_{20,w})[v_2/(v_2 + \delta_1 v_1)]^{1/3}$, where s_o is the sedimentation coefficient calculated for an unhydrated sphere with mass equal to that of the $DnaK_{ATPase}$ and is given by the relationship $s_o = M(1 - v_2\rho)/(6N\pi\eta R_o)$, where $R_o = [3Mv_2/(4\pi N)]^{1/3}$ and N is Avogadro's number. Axial ratios (a/b) of the equivalent ellipsoids of revolution were computed using Perrin's equation.

Acknowledgements

The authors gratefully acknowledge the support of the NSF (BIR-951360 to W.F.S.) and the NIH (R01-GM58256 to C.J.H.). Peter Sherwood, Knut Langsetmo, David Jeruzalmi, and Andrew Bohm are thanked for their many contributions to this project.

References

1. Hartl, F. U. & Hayer-Hartl, M. (2002). Molecular chaperones in the cytosol: from nascent chain to folded protein. *Science*, **295**, 1852–1858.
2. Bukau, B. & Horwich, A. L. (1998). The Hsp70 and Hsp60 chaperone machines. *Cell*, **92**, 351–366.
3. Lund, P. (2001). Microbial molecular chaperones. *Advan. Microbiol. Physiol.* **44**, 93–140.
4. Harrison, C. J. (2003). GrpE, a nucleotide exchange factor for DnaK. *Cell Stress Chaperones*, **8**, 218–224.
5. Packschies, L., Theyssen, H., Buchberger, A., Bukau, B., Goody, R. S. & Reinstein, J. (1997). GrpE accelerates nucleotide exchange of the molecular chaperone DnaK with an associative displacement mechanism. *Biochemistry*, **36**, 3417–3422.
6. Grimshaw, J. P., Jelesarov, I., Schonfeld, H. J. & Christen, P. (2001). Reversible thermal transition in GrpE, the nucleotide exchange factor of the DnaK heat-shock system. *J. Biol. Chem.* **276**, 6098–6104.
7. Grimshaw, J. P., Jelesarov, I., Siegenthaler, R. K. & Christen, P. (2003). Thermsosensor action of GrpE: the DnaK chaperone system at heat shock temperatures. *J. Biol. Chem.* **278**, 19048–19053.
8. Brehmer, D., Rudiger, S., Gassler, C. S., Klostermeier, D., Packschies, L., Reinstein, J. *et al.* (2001). Tuning of chaperone activity of Hsp70 proteins by modulation of nucleotide exchange. *Nature Struct. Biol.* **8**, 427–432.
9. Harrison, C. J., Hayer-Hartl, M., Di Liberto, M., Hartl, F. & Kuriyan, J. (1997). Crystal structure of the nucleotide exchange factor GrpE bound to the ATPase domain of the molecular chaperone DnaK. *Science*, **276**, 431–435.
10. Mally, A. & Witt, S. N. (2001). GrpE accelerates peptide binding and release from the high affinity state of DnaK. *Nature Struct. Biol.* **8**, 254–257.
11. Mehl, A. F., Heskett, L. D. & Neal, K. M. (2001). A GrpE mutant containing the NH(2)-terminal "tail"

region is able to displace bound polypeptide substrate from DnaK. *Biochem. Biophys. Res. Commun.* **282**, 562–569.
12. Janin, J. (1995). Principles of protein–protein recognition from structure to thermodynamics. *Biochimie*, **77**, 497–505.
13. Lo Conte, L., Chothia, C. & Janin, J. (1999). The atomic structure of protein–protein recognition sites. *J. Mol. Biol.* **285**, 177–198.
14. Klebe, C., Prinz, H., Wittinghofer, A. & Goody, R. S. (1995). The kinetic mechanism of ran—nucleotide exchange catalyzed by Rcc1. *Biochemistry*, **34**, 12543–12552.
15. Bogan, A. A. & Thorn, K. S. (1998). Anatomy of hot spots in protein interfaces. *J. Mol. Biol.* **280**, 1–9.
16. Wells, J. A. (1996). Binding in the growth hormone receptor complex. *PNAS*, **93**, 1–6.
17. Li, Y., Urrutia, M., Smith-Gill, S. J. & Mariuzza, R. M. (2003). Dissection of binding interactions in the complex between the anti-lysozyme antibody HyHEL-63 and its antigen. *Biochemistry*, **42**, 11–22.
18. Flaherty, K., Wilbanks, S., DeLuca-Flaherty, C. & McKay, D. (1994). Structural basis of the 70-kilodalton heat shock cognate protein ATP hydrolytic activity. II. Structure of the active site with ADP or ATP bound to wild type and mutant ATPase fragment. *J. Biol. Chem.* **269**, 12899–12907.
19. Gelinas, A. D., Langsetmo, K., Toth, J., Bethoney, K. A., Stafford, W. F. & Harrison, C. J. (2002). A structure-based interpretation of *E-coli* GrpE thermodynamic properties. *J. Mol. Biol.* **323**, 131–142.
20. Perkins, S. J. (1986). Protein volumes and hydration effects. The calculations of partial specific volumes, neutron scattering matchpoints and 280-nm absorption coefficients for proteins and glycoproteins from amino acid sequences. *Eur. J. Biochem.* **157**, 169–180.
21. Stafford, W. F. (1992). boundary analysis in sedimentation transport experiments: a procedure for obtaining sedimentation coefficient distributions using the time derivative of the concentration profile. *Anal. Biochem.* **203**, 295–301.
22. Gelinas, A. D., Toth, J., Bethoney, K. A., Langsetmo, K., Stafford, W. F. & Harrison, C. J. (2003). Thermodynamic linkage in the GrpE nucleotide exchange factor, a molecular thermosensor. *Biochemistry*, **42**, 9050–9059.
23. DeLano, W. L. (2002). Unraveling hot spots in binding interfaces: progress and challenges. *Curr. Opin. Struct. Biol.* **12**, 14–20.
24. Buchberger, A., Schroder, H., Buttner, M., Valencia, A. & Bukau, B. (1994). A conserved loop in the ATPase domain of the Dnak chaperons is essential for stable binding of GrpE. *Nature Struct. Biol.* **1**, 95–101.
25. Kuntz, I. D. & Kauzman, W. (1974). Hydration of proteins and polypeptides. *Advan. Protein Chem.* **28**, 239–345.
26. Cann, J. R. (1970). *Interacting Macromolecules*, Academic Press, New York.
27. Rivas, G., Stafford, W. & Minton, A. P. (1999). Characterization of heterologous protein–protein interactions using analytical ultracentrifugation. *Methods*, **19**, 194–212.
28. Stafford, W. F. & Sherwood, P. J. (2004). Analysis of heterologous interacting systems by sedimentation velocity: curve fitting algorithms for estimation of sedimentation coefficients, equilibrium, and kinetic constants. *Biophys. Chem.* **108**, 231–243.
29. Garcia de la Torre, J., Navarro, S., Lopez Martinez, M. C., Diaz, F. G. & Lopez Cascales, J. J. (1994). HYDRO: a computer program for the prediction of hydrodynamic properties of macromolecules. *Biophys. J.* **67**, 530–531.
30. Sheinerman, F. B. & Honig, B. (2002). On the role of electrostatic interactions in the design of protein-protein interfaces. *J. Mol. Biol.* **318**, 161–177.
31. Lee, L. P. & Tidor, B. (2001). Optimization of binding electrostatics: charge complementarity in the barnase-barstar protein complex. *Protein Sci.* **10**, 362–377.
32. Flaherty, K. M., DeLuca-Flaherty, C. & McKay, D. B. (1990). Three-dimensional structure of the ATPase of a 70 K heat-shock cognate protein. *Nature*, 346.
33. Kraulis, P. (1991). Molscript: a program to produce both detailed and schematic plots of protein structures. *J. Appl. Crystallog.* **24**, 946–950.

Edited by F. Schmid

(Received 2 February 2004; received in revised form 11 March 2004; accepted 29 March 2004)